12-15-2005

Control of Dispersion in Form Birefringent-Based Holographic Optical Retarders

Erica N. Montach
Kent State University - Kent Campus, erica.montbach@kodak.com

Philip J. Bos
Kent State University - Kent Campus, pbos@kent.edu

Optical Engineering 44(12), 124001 (December 2005)

Control of dispersion in form birefringent-based holographic optical retarders

Erica N. Montbach*
Philip J. Bos
Kent State University
Liquid Crystal Institute
Kent, Ohio 44240
E-mail: erica.montbach@kodak.com

Abstract. Holographic retarders based on form birefringence are shown to have controllable dispersion properties. Significantly, we show that the dispersion properties of these retarders can be adjusted over a large wavelength range by varying the periodicity of the index of refraction profile. These retarders with controllable dispersion characteristics are of high value for applications such as the compensation of liquid crystal displays.
[DOI: 10.1117/1.2148887]

Subject terms: hologram; form birefringence; Berreman 4×4 method; liquid crystal; birefringence.

Paper 040813R received Nov. 1, 2004; revised manuscript received Apr. 3, 2005; accepted for publication May 11, 2005; published online Jan. 4, 2006.

1 Introduction

Optical retarders are generally produced from homogeneous crystals or stretched polymer films. The birefringence and dispersion properties of these films are primarily controlled by the molecular structure of the material. Unfortunately, the resulting properties may not be what are desired for a particular application. For example, in the case where retardation films are designed to compensate liquid crystals for improved display devices, the dispersion characteristics of the retarder often do not match that of the liquid crystal. However, retarders based on form birefringence have the potential for greater control of material properties, such as dispersion. Additionally, holographic form birefringent retarders have been considered by other authors for compensation of liquid crystal displays.[1]

Anisotropy can result in molecularly isotropic materials when there is a modulation of the refractive index, and the periodicity of that modulation is small compared to the illuminating wavelength of light.[2] This phenomenon is known as form birefringence. In the form birefringent regime, diffractions of higher orders are evanescent; therefore, only the zeroth-order diffraction exits the grating.[3] The grating acts as a negative uniaxial retarder with the optic axis perpendicular to the index modulation.

The retardation value of simple holograms in the form birefringence regime has been theoretically predicted for both the square-wave dielectric profile and the sine-wave dielectric profile. The term simple hologram refers to a volume index modulated grating. This type of simple hologram is made by imaging either a reflector or diffuser and the method used for creating these simple holograms is reviewed in Ref. 4. This results in a structure that has layers of varying indices of refraction through the thickness of the film. In this paper, we investigate when the index varies as either a sinusoidal or square function. The predicted ordinary and extraordinary index of refraction values for the simulated negative uniaxial film due to a square-wave variation of the isotropic hologram index are shown in the following equations[3,5]:

$$n_o = \left[\frac{(n_1^2 + n_2^2)}{2} \right]^{1/2}, \tag{1}$$

$$n_e^{\text{square}} = \sqrt{\frac{2n_1^2 n_2^2}{(n_1^2 + n_2^2)}} \tag{2}$$

where n_1 is the index of one of the alternating layers, n_2 is the index of the other, n_o is the ordinary index of the simulated uniaxial material, and n_e is the extraordinary index of the simulated uniaxial material. For Eqs. (1) and (2) to be valid, the hologram's isotropic index must vary with a periodicity much less than the wavelength of light. The predicted ordinary and extraordinary index of refraction values for the simulated negative uniaxial film due to a sine wave variation of the hologram's isotropic index are[3,6]

$$n_e^{\text{sin}} = n_o - \frac{(n_1 - n_2)^2}{n_1 + n_2}, \tag{3}$$

$$\Delta n^{\text{sin}} = n_e - n_o = \frac{(n_1 - n_2)^2}{n_1 + n_2}, \tag{4}$$

where Δn is the birefringence or difference between the ordinary and extraordinary indices of the simulated uniaxial material. Once again for Eqs. (3) and (4) to be valid, the hologram's isotropic index must vary with a periodicity much less than the wavelength of light. Onedraw back to Eqs. (1), (2), (3), and (4) is that they do not allow for consideration of the effect of variations in the functional profile of the hologram's isotropic index or for the dispersion of the simulated ordinary and extraordinary indices with respect to the wavelength of light.

In this paper, we will use the Berreman 4×4 matrix method[7] to calculate the phase shift and retardation of form

*Current location, Eastman Kodak, 1999 Lake Ave., B-82A, Rochester, New York 14650-2109.

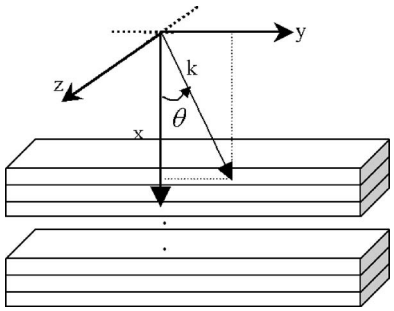

Fig. 1 Berreman discretization and axes definition. The dielectric permittivity tensor varies from layer to layer but within each layer it is constant.

birefringent retarders. The hologram's isotropic index periodicities and the functional profiles of the hologram are varied. Additionally, the angle of incidence with respect to the hologram's surface normal and the incident wavelength of light is also varied. We also demonstrate for the first time the ability to tune the dispersion of these types of retarders.

2 Calculation of Phase Retardation

To compute the phase retardation of form birefringent retarders we used the Berreman 4×4 matrix method.[8] This method, described in detail by many authors,[9,10] enables calculation of the reflected and transmitted s and p waves from a medium where the index of refraction profile varies only along one direction. The medium is discretized into layers that are thin enough so that variations in the index of refraction are negligible within them.

The 4×4 matrix method solves Maxwell's equations for anisotropic media with no free charges.[10] The electric and magnetic field vectors are assumed to be plane waves. The calculation is simplified by defining the wave vector in only the xy plane (Fig. 1); any other orientation can be created by simply rotating the axes frame. Two of Ampere's and Faraday's laws can be rewritten in matrix form:

$$\begin{pmatrix} 0 & 0 & ik_y \\ 0 & 0 & -\frac{\mathrm{d}}{\mathrm{d}x} \\ -ik_y & \frac{\mathrm{d}}{\mathrm{d}x} & 0 \end{pmatrix} \begin{pmatrix} E_x \\ E_y \\ E_z \end{pmatrix} = \boldsymbol{ik}_o z_o \begin{pmatrix} H_x \\ H_y \\ H_z \end{pmatrix}, \tag{5}$$

$$\begin{pmatrix} 0 & 0 & ik_y \\ 0 & 0 & -\frac{\mathrm{d}}{\mathrm{d}x} \\ -ik_y & \frac{\mathrm{d}}{\mathrm{d}x} & 0 \end{pmatrix} \begin{pmatrix} H_x \\ H_y \\ H_z \end{pmatrix} = -i\frac{\boldsymbol{k}_o}{z_o} \begin{pmatrix} \epsilon_{xx}E_x + \epsilon_{xy}E_y + \epsilon_{xz}E_z \\ \epsilon_{yx}E_x + \epsilon_{yy}E_y + \epsilon_{yz}E_z \\ \epsilon_{zx}E_x + \epsilon_{zy}E_y + \epsilon_{zz}E_z \end{pmatrix}, \tag{6}$$

where the constant z_o is the impedance of vacuum, $\mathbf{E}$ is the electric field vector, ϵ_{ij} (where i and j are replaced by x, y, or z) are the dielectric permittivity tensor components, and k_o is the wave vector in vacuum. Equations (5) and (6) represent six equations in which two of those equations are independent of derivatives. The tangential components E_y, H_y, E_z, and H_z are continuous across boundaries while the normal components E_x and H_x may be discontinuous.[11] Since the normal components may be discontinuous across boundaries, they are eliminated from the matrix calculation by substitution using the two equations that do not contain derivatives. This substitution results in the following four equations:

$$\frac{\mathrm{d}}{\mathrm{d}x} \begin{pmatrix} E_y \\ H_z \\ E_z \\ -H_y \end{pmatrix} = \boldsymbol{ik}_o \begin{bmatrix} -\beta\frac{\epsilon_{xy}}{\epsilon_{xx}} & z_o\left(1-\frac{\beta^2}{\epsilon_{xx}}\right) & -\beta\frac{\epsilon_{xz}}{\epsilon_{xx}} & 0 \\ \frac{1}{z_o}\left(\epsilon_{yy}-\frac{\epsilon_{xy}^2}{\epsilon_{xx}}\right) & -\beta\frac{\epsilon_{xy}}{\epsilon_{xx}} & \frac{1}{z_o}\left(\epsilon_{yz}-\frac{\epsilon_{xy}\epsilon_{xz}}{\epsilon_{xx}}\right) & 0 \\ 0 & 0 & 0 & z_o \\ \frac{1}{z_o}\left(\epsilon_{yz}-\frac{\epsilon_{xy}\epsilon_{xz}}{\epsilon_{xx}}\right) & -\beta\frac{\epsilon_{xz}}{\epsilon_{xx}} & \frac{1}{z_o}\left(\epsilon_{zz}-\frac{\epsilon_{xz}^2}{\epsilon_{xx}}-\beta^2\right) & 0 \end{bmatrix} \times \begin{pmatrix} E_y \\ H_z \\ E_z \\ -H_y \end{pmatrix}, \tag{7}$$

This is rewritten as

$$\boldsymbol{\psi}' = \nabla\boldsymbol{\psi}, \tag{8}$$

where the vector $\boldsymbol{\psi}$ is the tangential field vector shown in Eq. (7), $\beta = n\sin(\theta)$, n is the index of the initial material, θ is the angle of incidence with respect to the hologram surface, and the matrix ∇ is the 4×4 matrix shown in Eq. (7) and is defined as the differential propagation matrix. Equation (8) is the differential equation that must be solved to complete the 4×4 matrix calculation.[12] One way to solve the differential equation in the 4×4 matrix method is to discretize the media into thin layers. This discretization method was originally developed by Berreman and Scheffer.[7] Each layer is assumed to have a constant dielectric permittivity tensor in all dimensions. Once the media is separated into layers, the differential equation in Eq. (8) is solved for layer by layer.[10] By repeating this matrix multiplication many layers can be accounted for, resulting in the following equation:

$$\boldsymbol{\psi}_{\mathrm{exit}} = \mathbf{M}_{\mathrm{layer\ N}} \cdots \mathbf{M}_{\mathrm{layer\ 2}} \mathbf{M}_{\mathrm{layer\ 1}} \boldsymbol{\psi}_{\mathrm{enter}}, \tag{9}$$

where $\mathbf{M}$ is the matrix propagating light from one layer to the next.[13] The operator matrix $\mathbf{M}$ is the integral solution of the operator matrix ∇.

We extracted the phase retardation of the periodic material by simulating polarized light propagation through the hologram and then directly calculating the phase shift between E_s and E_p. The incident light is polarized at 45 deg, where the polarization plane is defined on axis as 45 deg from the plane of incidence. For this simplified explanation,

H_z and H_y are set equal to zero just to enable multiplication to be carried through resulting in the following starting vector for Eq. (9):

$$\boldsymbol{\psi}_{\text{enter}} = \frac{1}{\sqrt{2}}\begin{pmatrix} 1 \\ 0 \\ 1 \\ 0 \end{pmatrix}. \tag{10}$$

The phase retardation is ultimately calculated from the output field vector $\boldsymbol{\psi}_{\text{exit}}$. Recall that the output field vector contains orthogonal electric field components E_p and E_s and the phase shift between those components results in the phase retardation. The phase retardation (also referred to as phase shift) Γ is found with the following equation.

$$\Gamma = a\tan\left[\frac{\text{imag}(E_p/E_s)}{\text{real}(E_p/E_s)}\right] = \frac{2\pi\Delta nd}{\lambda_0}, \tag{11}$$

where Δn is the birefringence of the form birefringent hologram, d is the thickness of the hologram, and λ_0 is the wavelength in vacuum. The path length retardation (also referred to as retardation) R is found with the following equation.

$$R = \frac{\Gamma\lambda_0}{2\pi}. \tag{12}$$

3 Effect of Hologram Periodicity on Form Birefringence

To calculate the effect on the phase shift from varying the periodicity of a form birefringent hologram, we considered the cases where the index of refraction had a sine wave variation[14]:

$$n = \left[\left(\frac{n_1 - n_2}{2}\right) + \left(\frac{n_1 + n_2}{2}\right)\cos(\boldsymbol{K} \square \boldsymbol{x})\right], \tag{13}$$

where $\boldsymbol{K}$ is the grating vector and $\boldsymbol{x}$ is the location in the depth of the simple hologram. For a square-wave variation the index function is

$$n = \begin{cases} n_1 \;\; N = 1,3,\ldots \\ n_2 \, N = 2,4,\ldots, \end{cases} \tag{14}$$

where N is the number of the sheet having one isotropic index. The discretized layers of the Berreman method previously mentioned are much thinner then one period of the hologram, in other words a sheet is not equal to a layer. Applying the Berreman method, we divide the index profile into enough layers so that the modeled results will simulate continuous index in each layer; 2000 layers for the sinusoidal profile and less for the square profile.

In the following calculations, the angle of incidence is 60 deg to the surface normal, unless the parameter varied is incident angle. The incident angle used is 60 deg because that allows the two polarizations to "see" different indices of refraction as passing through the form birefringent hologram. The simulated optic axis is parallel to the film normal and on-axis light results in E_p and E_s "seeing" two equal indices of refraction, thus resulting in zero phase shift. In the following calculations, the wavelength is 550 nm, unless the varied parameter is wavelength. The material surrounding the hologram is isotropic and has an index value that minimizes specular reflections, $n=1.5$. The incident and exiting electric fields are defined in the surrounding isotropic media, which is on both sides of the material of interest. The hologram investigated has $n_1=1.595$, $n_2=1.449$, $d=45.2$ μm, a sine wave dielectric profile[6] (unless otherwise stated), and unslanted layers that are parallel to the surface.

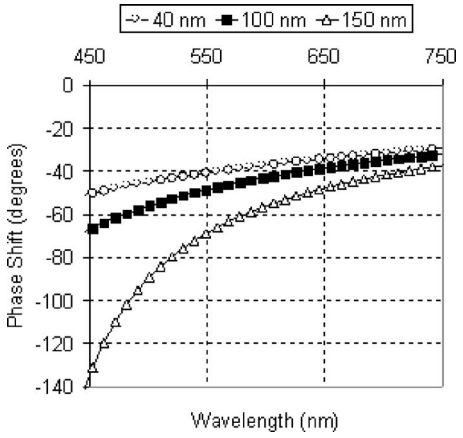

Fig. 2 Phase shift versus wavelength for various hologram periodicities, labeled at the top of the graph. All holograms have the sine wave dielectric profile. Incident angle is 60 deg. Theoretical results.

A main point of the paper is that the wavelength dispersion of birefringence for form birefringent holograms can be tuned by varying the hologram's periodicity. As the hologram's periodicity increases, the range of retardation values increases also. This continues until the hologram reaches the Bragg regime. Samples of the possible wavelength dispersions are shown in Fig. 2 (Fig. 3 shows the reflectance spectra for the holograms used in Fig. 2) and Fig. 4. Figure 2 demonstrates that as the hologram's periodicity increases the phase shift from the hologram also increases. Figure 4 reveals that the wavelength dispersion of birefringence is unaltered as the dielectric profile is

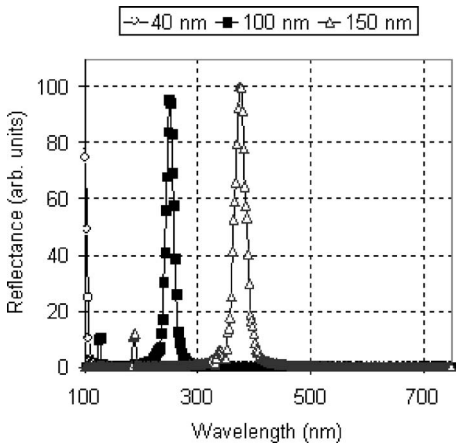

Fig. 3 Reflectance versus wavelength for the holograms used in Fig. 2, with a 60 deg incident angle. Theoretical results.

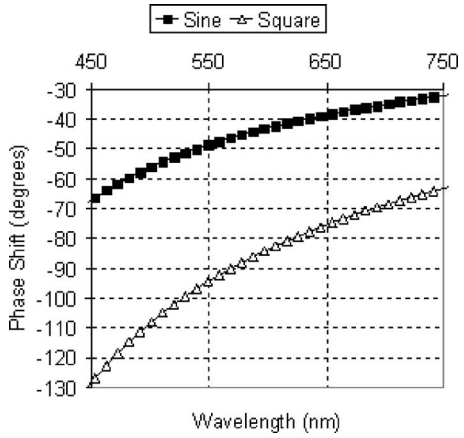

Fig. 4 Phase shift versus wavelength for two different functional forms of the hologram's dielectric profile, labeled at the top of the graph. All holograms have a 100 nm periodicity; 60 deg incident angle. Theoretical results.

changed; therefore, the same wavelength dispersion could be attained using a compensator with a square-wave dielectric profile as with a sine wave, but the square wave has the added advantage of a higher average birefringence. Figures 3 and 5 show the reflectance for the same holograms used in Figs. 2 and 4. The visible spectrum is well beyond the Bragg regime for each of the holograms considered. All graphical results are obtained by theoretical calculation of light propagation through the optical media of interest using the Berreman 4×4 matrix method as described earlier and in Ref. 14.

The plot in Fig. 6 shows the variation in retardation as a function of wavelength divided by the periodicity of the hologram. Three plots for different periodicities are shown in Fig. 6. Notice that once the wavelength is normalized to the periodicity all plots coincide; therefore, the periodicity of the hologram behaves as a scaling factor for the wavelength of incident light. Also, the retardation of all holograms enters the form birefringent regime when the periodicity is approximately the wavelength divided by 10. We assume an ordinary index of refraction $n_o=1.5237$, and calculate the extraordinary index of refraction. In Fig. 6 the retardation in the limit of a large wavelength/period ratio is −63 nm. This yields a calculated birefringence of $\Delta n^{\sin}_{\text{Berreman}}=-0.0035$, which agrees well with the predicted value found from Eq. (4), $\Delta n^{\sin}_{\text{Calc}}=-0.0035$.

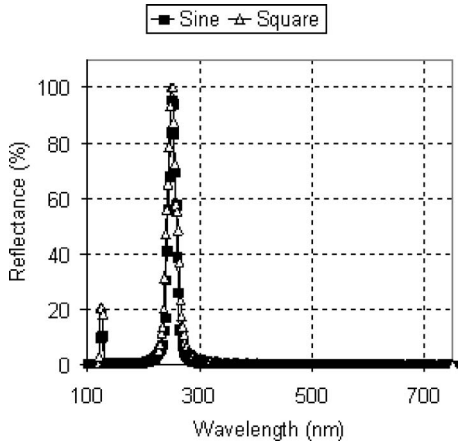

Fig. 5 Reflectance versus wavelength for the holograms used in Fig. 4; 60-deg incident angle. Theoretical results.

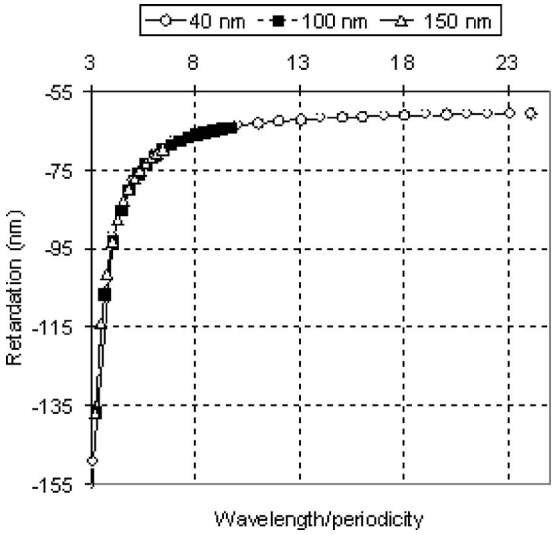

Fig. 6 Retardation versus wavelength divided by the periodicity of each hologram. There are three holograms with periodicities equal to 40, 100, and 150 nm. Holograms have a sine wave dielectric profile. Light is incident at 60 deg. Theoretical results.

Using the calculated birefringence values of the form birefringent hologram, a negative birefringent retarder is engineered with the exact same birefringence. A negative birefringent retarder is similar to a negative uniaxial crystal,[15] except the retarder is not restricted to crystalline form but can also be a polymer film with oriented molecules. The calculated phase retardation of the form birefringent hologram and the engineered negative birefringent retarder are compared in Fig. 7 and very good agreement is seen between the two. This demonstrates that the form birefringent hologram does behave as a linear retarder.

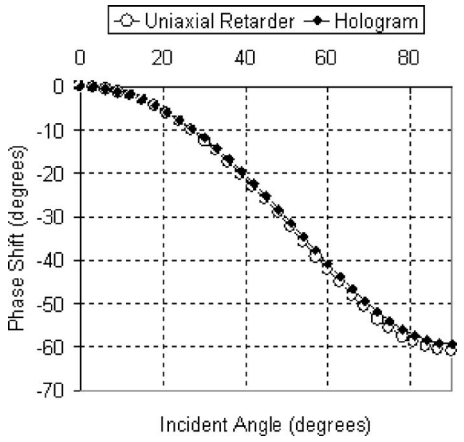

Fig. 7 Phase shift versus incident angle (with respect to the surface of the hologram) for both a uniaxial retarder and a form birefringent hologram with a sine wave dielectric profile. The parameters of the uniaxial retarder are $n_o=1.5237$, $n_e=1.5202$, $d=45.2$ mm, and the optic axis is parallel to the film normal. Theoretical results.

4 Tuning the Wavelength Dependence of Birefringence

To demonstrate that a form birefringent hologram can have its dispersion tuned to match the dispersion of the liquid crystal material (defined as a matched-dispersion retarder), and that the matched-dispersion retarder compensates more effectively, we will consider a vertically aligned LCD (VA LCD). A VA LCD has the liquid crystal (LC) molecules oriented so that their average effective optic axis is parallel to the layer normal when a voltage is not applied to a pixel. Once a voltage above a certain threshold is applied to the VA LCD pixel, the molecules begin to orient so that their average effective optic axis is perpendicular to the layer normal. If the polarizers of the display are crossed then in the off state the pixel blocks light and appears black, while when a voltage is applied above a certain threshold, the pixel allows light through and appears bright.[16] Therefore, a negative birefringent retarder with its optic axis parallel to the layer normal, such as the form birefringent holograms described here, would ideally compensate the VA LCD. The LCD consists of crossed polarizers, an LC in the VA mode, and a compensator. The form birefringent hologram compensates the LC in its unperturbed state. The LC material modeled is MLC-6608, its Cauchy coefficients are $A_o=1.4643$, $B_o=3995$ nm^2, $A_e=1.5370$, and $B_e=7509$ nm^2; the dielectric constants are $\epsilon_{\|}=3.6$ and $\epsilon_{\perp}=7.8$; and the elastic constants are $k_{11}=16.7$ pN and $k_{33}=18.1$ pN. The LCD has a 90-deg pretilt and the cell is 3.26 μm thick.

The form birefringent hologram used to compensate the liquid crystal has the material parameters described above where we used a 60-deg angle of incidence. The only deviations from that description are that the thickness is increased to 69 μm, so that the retardation of the hologram equals that of the LC layer, and the hologram's periodicity is 66 nm. The hologram's wavelength dispersion is tuned to match that of the LC by varying the hologram's periodicity. The first variable defined when designing the hologram required to compensate the LC is the total thickness. The thickness is found by matching the hologram's retardation to that of the LC's. The indices are already defined by the material parameters n_1 and n_2. After the thickness and indices are known, the hologram's periodicity is varied until the resulting path length retardation of the hologram matches that of the LC for all wavelengths. The form birefringent hologram is compared with a standard homogeneous negative birefringent retarder made of discotic LCs. We refer to this standard homogeneous retarder as the DLC retarder. The optic axis of the considered DLC negative birefringent retarder is parallel to the film normal (negative *c*-plate); its estimated Cauchy coefficients are $A_o=1.5441$, $B_o=5163.4$ nm^2, $A_e=1.5$, and $B_e=0$ nm^2 and the thickness is 4.47 μm.

The dispersion of the form birefringent hologram is shown to match that of the VA LCD in Fig. 8, while the dispersion of the negative *c*-plate has a greater variation with wavelength. Figures 9 and 10 show the transmission through the LCD compensated with either the form birefringent hologram or the DLC negative *c*-plate for 30 and 60 deg off axis (recall we have optimized the compensator properties at the 60-deg angle). The transmission through crossed polarizers equals the transmission through the VA LCD compensated with the dispersion matched hologram at 60 deg off axis, demonstrating almost perfect compensation at this angle.

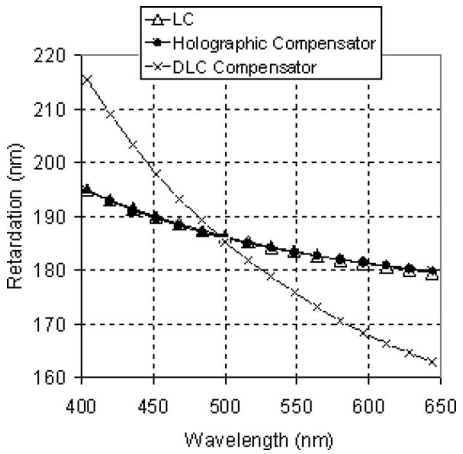

Fig. 8 Retardation versus wavelength. The incident angle is 60 deg. The retardation shown for both the form birefringent hologram and the DLC negative *c*-plate are the absolute value of the retardation, and the actual retardations for these two materials are negative. The absolute value of the retardation for the form birefringent hologram equals the retardation of the LC material. The dispersion of the DLC negative *c*-plate has a greater change with wavelength than the dispersion of the LC. Theoretical results.

5 Summary and Conclusion

We showed that holographic form birefringence retarders can be designed to have a desired dispersion of birefringence with respect to wavelength. This property is of high value in the design of compensators for LCDs. The previously known theoretical predicted values for the birefringence agrees well with the birefringence calculated using the Berreman method, once in the form birefringence regime. The dispersion of the hologram can be tuned by varying its periodicity until the Bragg regime is reached. The

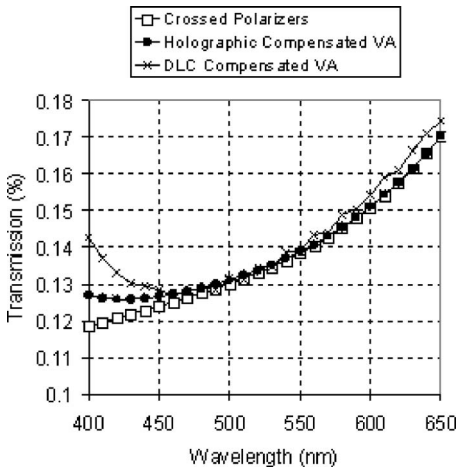

Fig. 9 VA LCD compensated with the dispersion matched form birefringent hologram has better performance than when compensated with the DLC negative *c*-plate at 30-deg indicent angle. The maximum transmission for the graph is 100. Theoretical results.

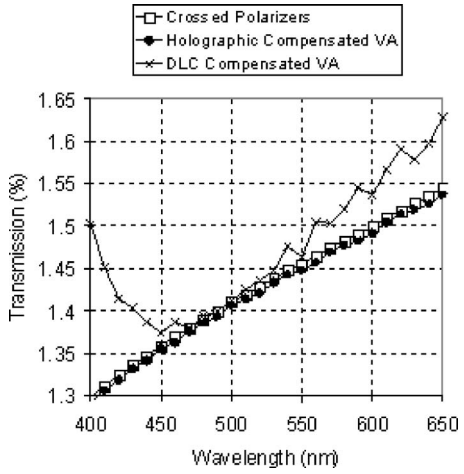

Fig. 10 VA LCD compensated with the dispersion matched form birefringent hologram has the same transmission as through crossed polarizers at 60-deg incident angle. The VA LCD compensated with the DLC negative *c*-plate has a higher transmission. The maximum transmission for the graph is 100. Theoretical results.

hologram's dispersion can be matched to a LC material's, enabling very good compensation; better than the currently available compensators.

Acknowledgments

This work was funded by DuPont Holographics and we would like to thank Dupont and William Gambogi for many helpful discussions.

References

1. C. Joubert and J.-C. Lehureau, "TN-LCD compensation film with holographic form birefringence," *Asia Displ.* 1119–1122 (1998).
2. M. Born and E. Wolf, *Principles of Optics*, 7th ed., pp. 826–827, Cambridge University Press, Cambridge (1999).
3. G. Campbell and R. K. Kostuk, "Effective-medium theory of sinusoidally modulated volume holograms," *J. Opt. Soc. Am. A* **12**(5), 1113–1117 (1995).
4. S. Stevenson, "DuPont multicolor holographic recording films," *Proc. SPIE* **2011**, 231–241 (1997).
5. J. P. Eblen, Jr., W. J. Gunning, J. Beedy, D. Taber, L. Hale, P. Yeh, and M. Khoshnevisan, "Birefringent compensators for normally white TN-LCDs," in *SID'94 Digest*, pp. 245–248 (1994).
6. T. J. Kim, G. Campbell, and R. K. Kostuk, "Volume holographic quarterwave plate," in Application and Theory of Periodic Structures, T. Jannson and N. C. Gallagher, Eds., *Proc. SPIE* **2532**, 15–22 (1995).
7. D. W. Berreman and T. J. Scheffer, *Mol. Cryst. Liq. Cryst.* **11**, 395 (1970).
8. D. W. Berreman, *SID'93 Digest* **24**, 101 (1993).
9. P. Yeh and C. Gu, *Optics of Liquid Crystal Displays*, Wiley, New York (1999).
10. I. J. Hodgkinson, *Birefringent Thin Films and Polarizing Elements*, World Scientific, Singapore (1997).
11. L. Solymar and D. J. Cooke, *Volume Holography and Volume Gratings*, Academic Press, New York (1981).
12. G. F. Barrick, PhD Dissertation, Department of Chemical Physics, Kent State University (2000).
13. G. F. Barrick, *SID 2002 Digest* **33**, 498 (2002).
14. E. N. Montbach, PhD Dissertation, Department of Chemical Physics, Kent State University (2003).
15. E. Hecht, *Optics*, 3rd ed., p. 337, Addison-Wesley, Reading, MA (1998).
16. V. A. Konovalov, A. A. Muravski, S. N. Timofeev, and S. Ye. Yakovendo, *SID 1999 Digest* **30**, 668–671 (1999).

Erica N. Montbach completed her PhD at the Liquid Crystal Institute (LCI), Kent State University, in 2003 on liquid crystals and holographic optical elements under the guidance of Dr. Philip J. Bos. She is currently a senior research scientist at Eastman Kodak. Prior to attending LCI, she received her BA in physics from the College of Wooster, where she completed her senior thesis on the electro-optics of smectic-A liquid crystals under the guidance of Dr. Shila Garg. She also completed her MS in physics at Colorado State University.

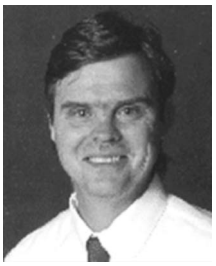

Philip J. Bos received his PhD degree in physics from Kent State University in 1978. After one year as a research fellow at the Liquid Crystal Institute at Kent State he joined Tektronix Laboratories in the Display Research Department. In 1994 he returned to the Liquid Crystal Institute, where he is currently an associate director and a professor of chemical physics. He currently has several projects in the area of applications of liquid crystals. He has over 100 publications and holds 20 patents.